Electronic Supplementary Material (ESI) for Analytical Methods.

Electronic Supplementary Information

The study of a novel high selectivity pyrenyl-based fluorescence probe for Fe^{3+} detection designed by structure modulation strategy

Sen Liu[1,2], Jun Li[1], Tianjiao Hou[1]* and Xuan Shen[1,2]*

1. State Key Laboratory of Materials-oriented Chemical Engineering, College of Chemical Engineering, Nanjing Tech University, Nanjing 211816, P. R. China.
2. Zhangjiagang Institute of Nanjing Tech University, Suzhou 215600, P. R. China.

*Corresponding Author E-mail: hou_tianjiao@njtech.edu.cn, shenxuan@njtech.edu.cn

Materials and reagents

1-Pyrenylboronic acid, 2-bromo-5-(trifluoromethyl)pyridine, 2-bromo-5-methylpyridine, and $Pd(PPh_3)_4$ were purchased from Shanghai Haohong Biomedical Technology Co., Ltd. NaOH, $FeCl_3$, $AlCl_3$, $FeCl_2{\cdot}4H_2O$, $CrCl_3{\cdot}6H_2O$, NaCl, $MgCl_2{\cdot}6H_2O$, $CuCl_2{\cdot}2H_2O$, $ZnCl_2$, $CaCl_2$, $MnCl_2$, $ZrCl_4$, $SrCl_2{\cdot}6H_2O$, $BaCl_2{\cdot}2H_2O$, $CdCl_2{\cdot}2.5H_2O$, $InCl_3$, $LiCl{\cdot}H_2O$, KNO_3, $AgNO_3$, $Co(NO_3)_2{\cdot}6H_2O$, $Pb(NO_3)_2$, $Ni(NO_3)_2{\cdot}6H_2O$, $Eu(NO_3)_3{\cdot}6H_2O$, $La(NO_3)_3$, $Er(NO_3)_3{\cdot}6H_2O$, $Tb(NO_3)_3{\cdot}6H_2O$, $Dy(NO_3)_3{\cdot}5H_2O$, $Sm(NO_3)_3$, $Y(NO_3)_3{\cdot}6H_2O$, $HgSO_4$, $KF{\cdot}2H_2O$, NaCl, NaBr, Na_2SO_4, Na_2SO_3, $NaHSO_3$, $NaHSO_4{\cdot}H_2O$, Na_2CO_3, $NaHCO_3$, CH_3COONa, KNO_3, $NaNO_2$, and $NaClO_4{\cdot}H_2O$ were purchased from Shanghai Lingfeng Chemical Reagent Co., Ltd. Hydrochloric acid and acetonitrile were purchased from Wuxi Yasheng Chemical Co., Ltd. Tris(hydroxymethyl) aminomethane was purchased from Shanghai Xushuo Biotechnology Co., Ltd. Silica gel (200-300 mesh) was purchased from Qingdao Dingkang silica gel Co., Ltd.

Instruments

^1H NMR, ^{13}C NMR, and ^{19}F NMR spectra were recorded on a Bruker AM 400 MHz in chloroform-d solution, and the tetramethylsilane (TMS) signal as an internal standard. FT-IR spectra were measured on a Thermo Nicolet 380 FT-IR spectrophotometer with KBr pellets at room temperature. The electrospray ionization mass spectra (ESI-MS) were accomplished by Agilent 6200 series TOF/6500 series. The crystallographic data were collected on a Bruker SMART APEX II CCD area detector diffractometer. UV-Vis absorbance spectra were measured by a SHIMADZU UV-3600 spectrophotometer. Fluorescence spectra were performed by using a Hitachi F-7000 fluorescence Spectrophotometer, and 350 nm was used as an excitation wavelength throughout the experiment (E_X Slit = 2.5 nm, E_M Slit = 5 nm). Particle size distribution analyses were performed by dynamic light scattering (DLS) measurements at room temperature on a Brookhaven 90Plus/BI-MAS (USA). Transition electron microscopy (TEM) images were recorded on a Hitachi H7700 at a voltage of 120 kV. Samples for the TEM studies were prepared by evaporating nanoparticle suspension that drop on copper grid. The pH values of solvent were adjusted by using pHS-3C pH meter. Time-resolved fluorescence decay curves and PLQY were measured on an Edinburgh FLS 980 fluorescence spectrometer.

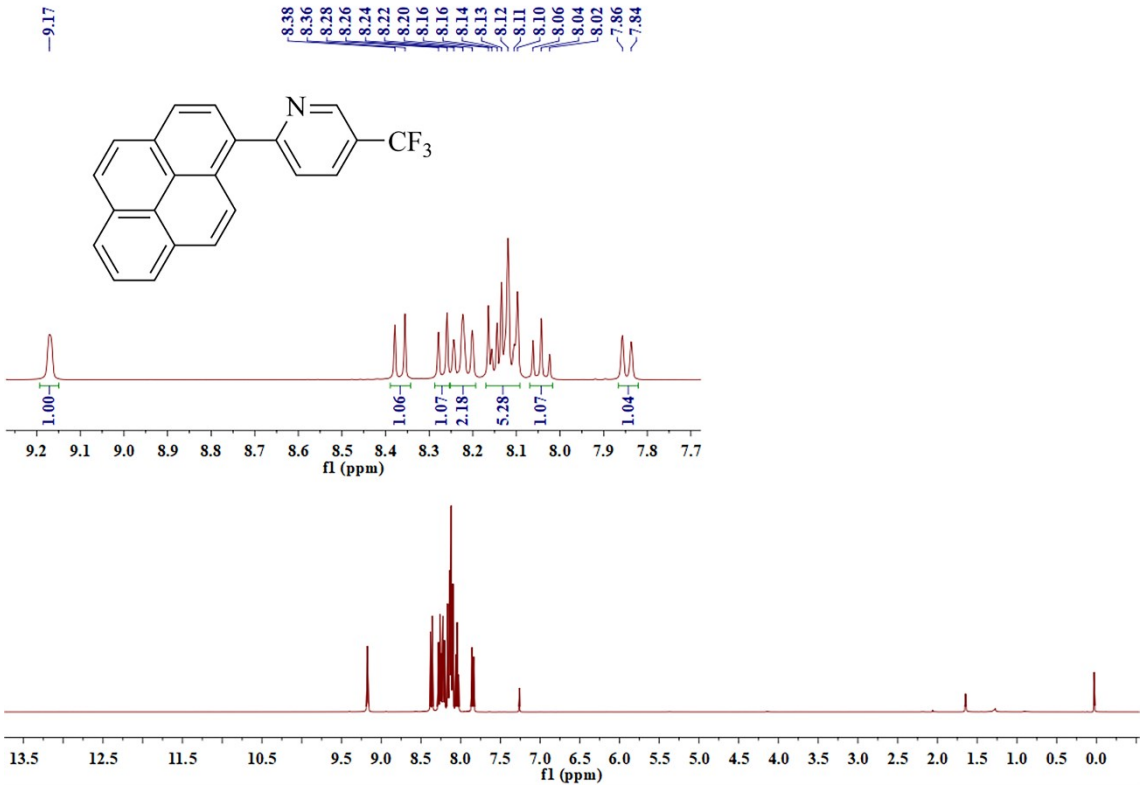

Fig. S1 The ^{1}H NMR spectrum of **pypyr-CF_3** in $CDCl_3$.

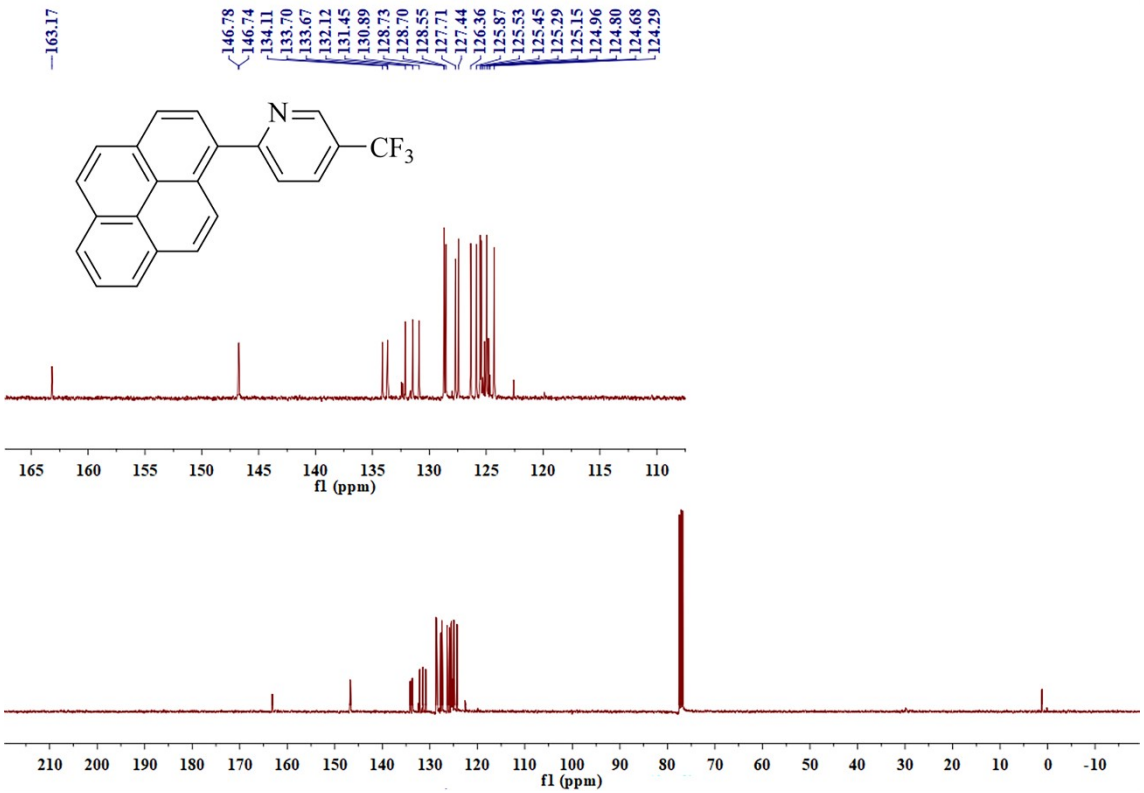

Fig. S2 The ^{13}C NMR spectrum of **pypyr-CF_3** in $CDCl_3$.

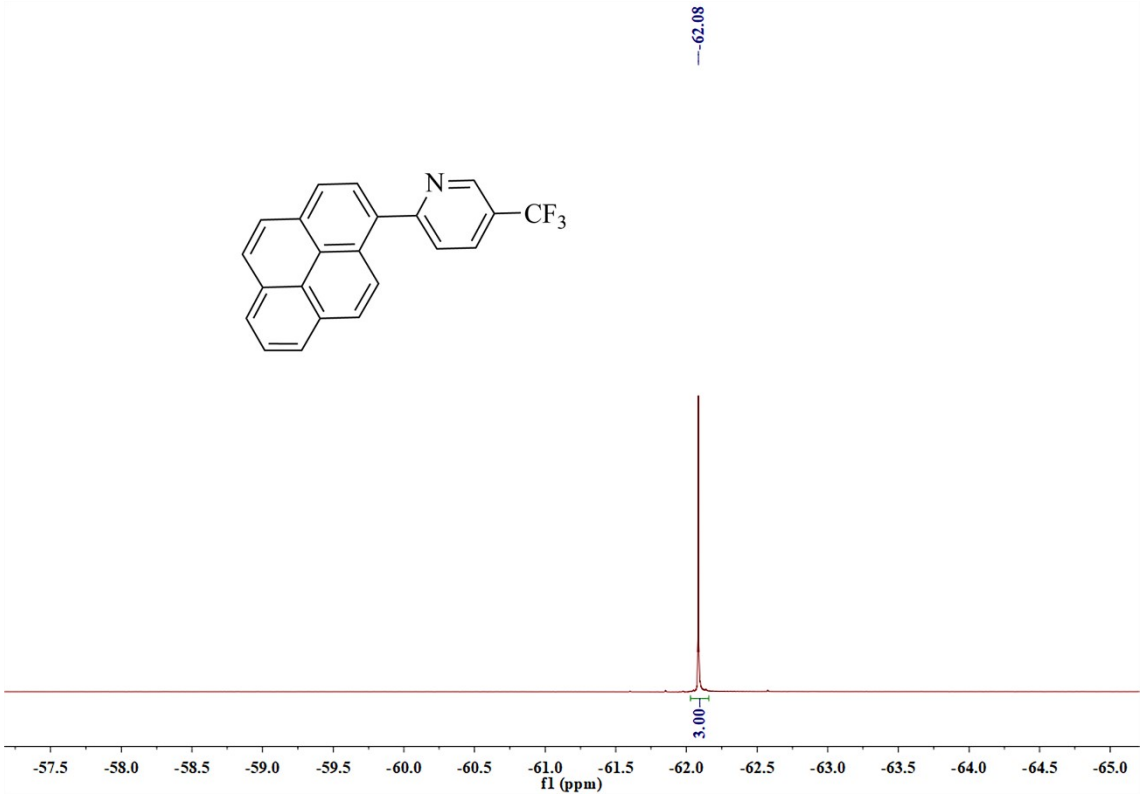

Fig. S3 The ^{19}F NMR spectrum of **pypyr-CF_3** in $CDCl_3$.

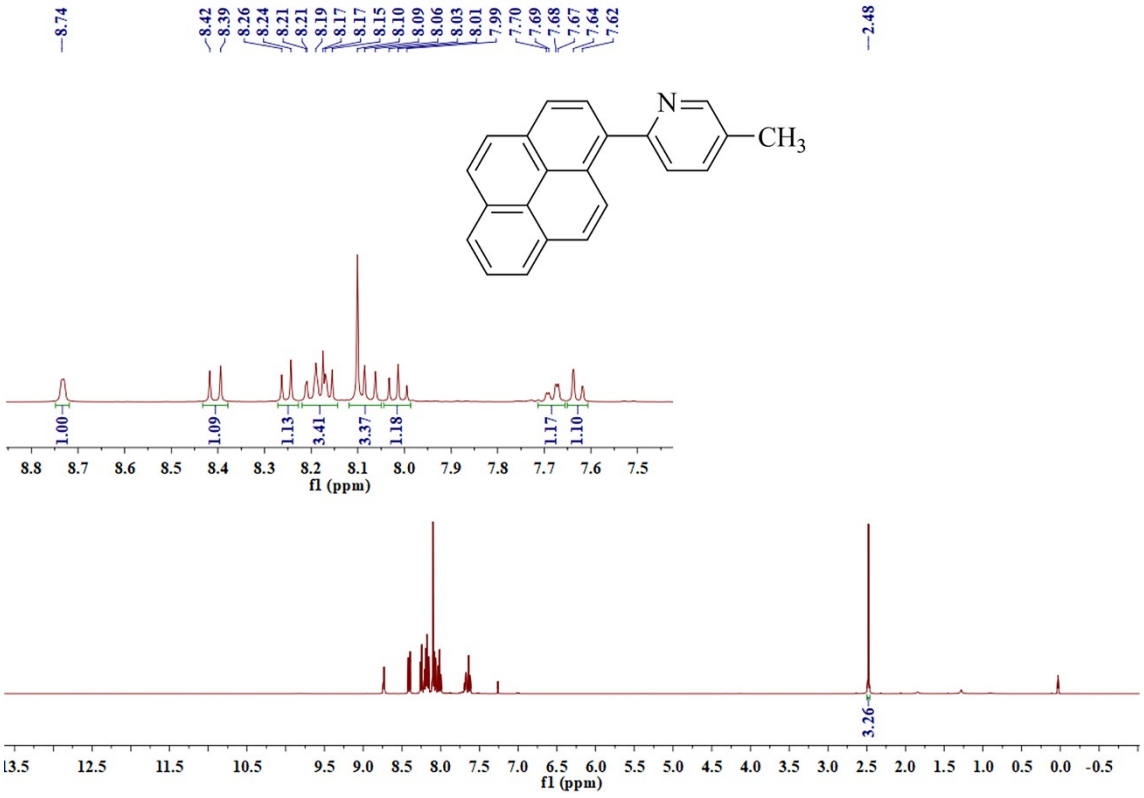

Fig. S4 The ^{1}H NMR spectrum of **pypyr-CH_3** in $CDCl_3$.

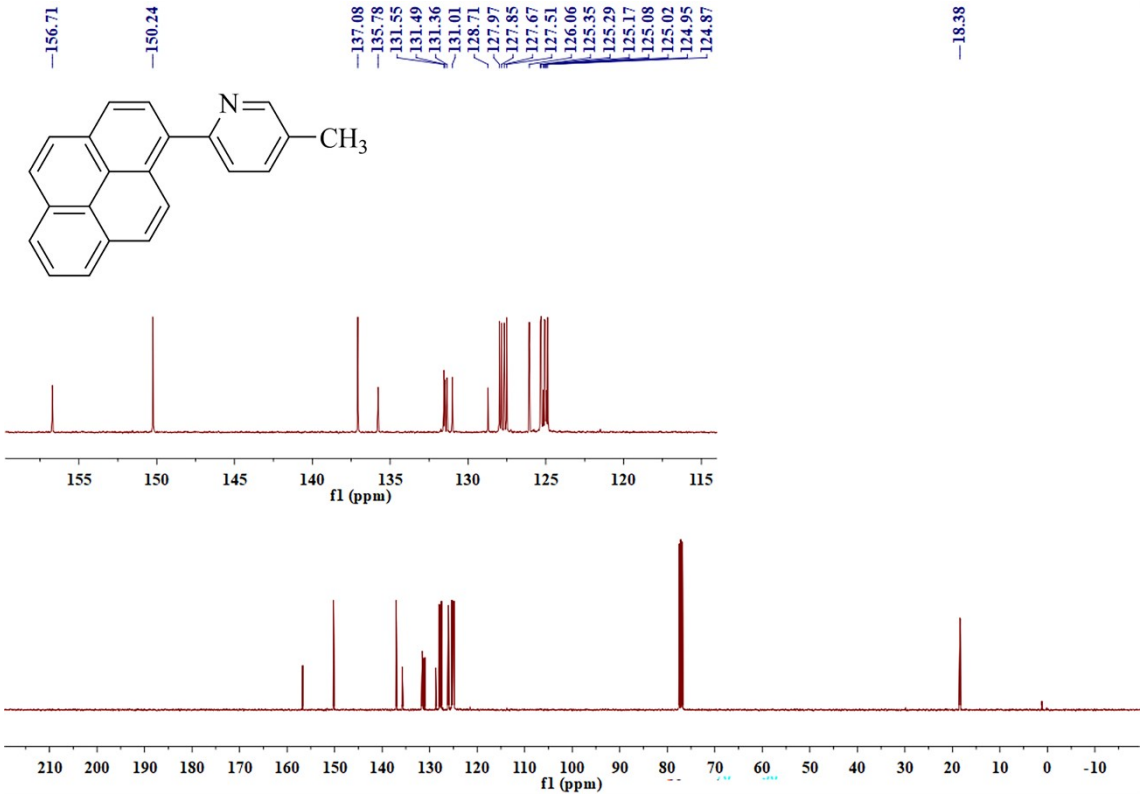

Fig. S5 The ^{13}C NMR spectrum of **pypyr-CH_3** in $CDCl_3$.

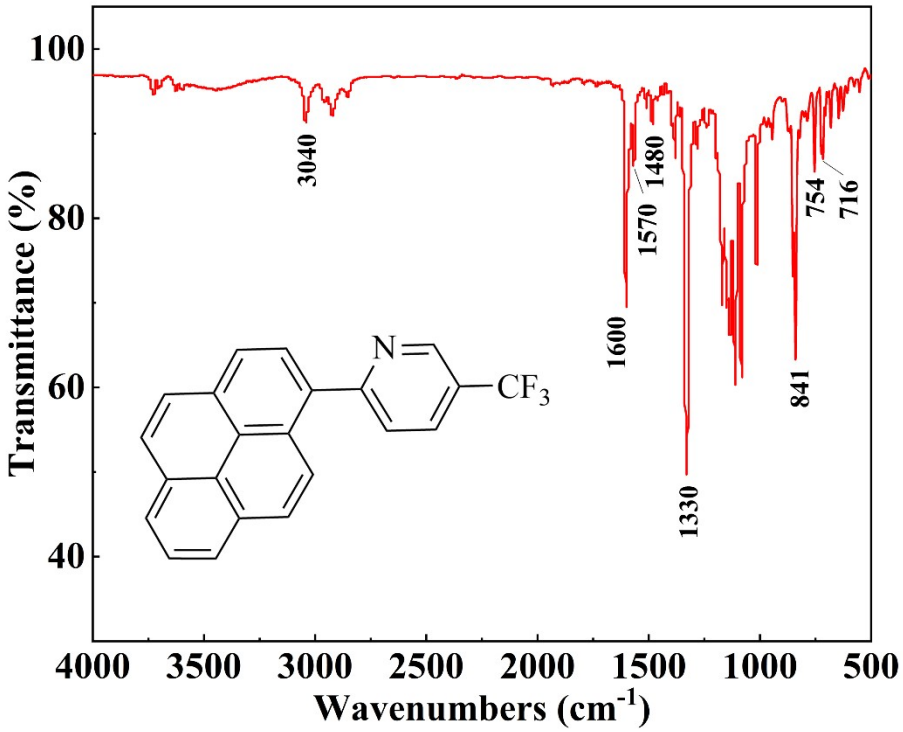

Fig. S6 The FT-IR spectrum of **pypyr-CF_3**.

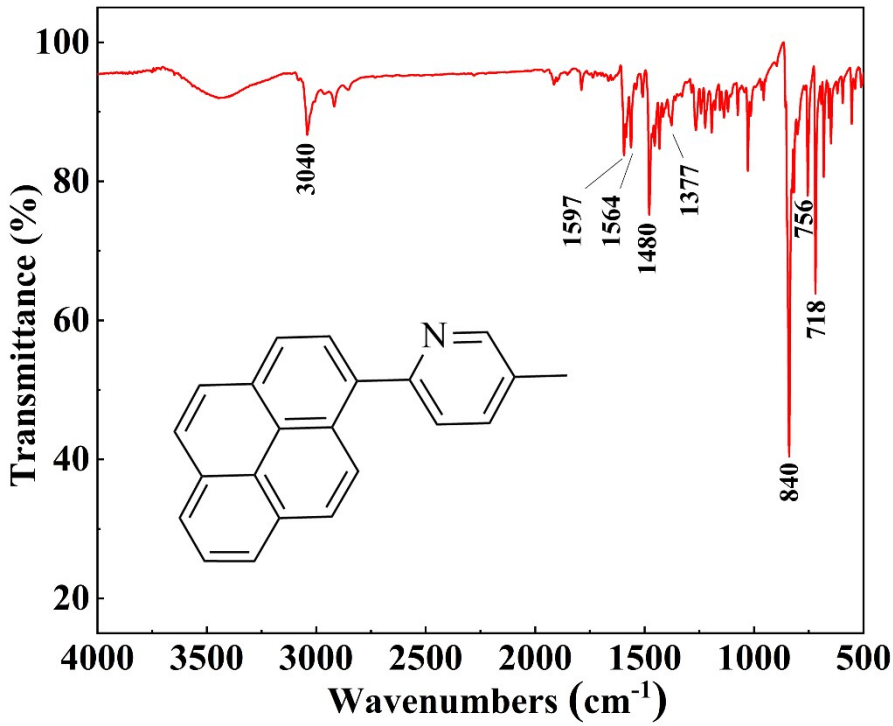

Fig. S7 The FT-IR spectrum of **pypyr-CH_3**.

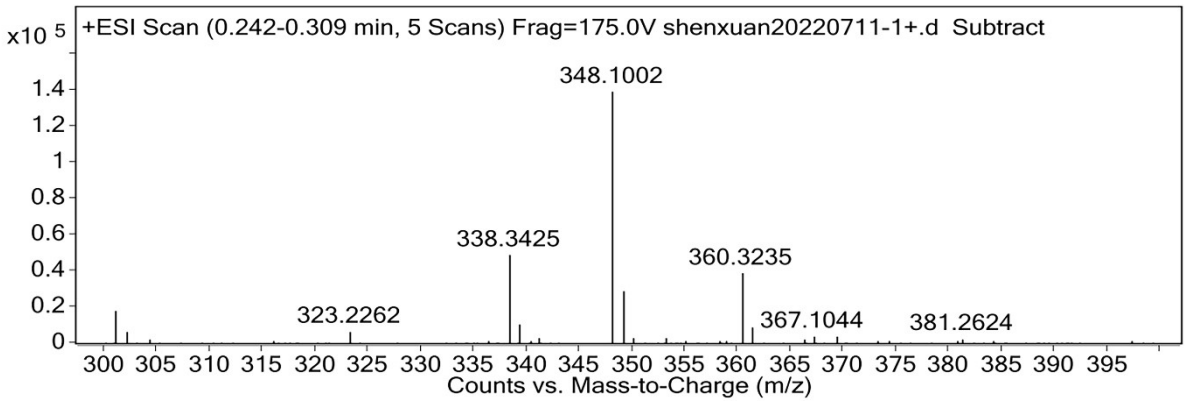

Fig. S8 The ESI-MS spectrum of **pypyr-CF_3**.

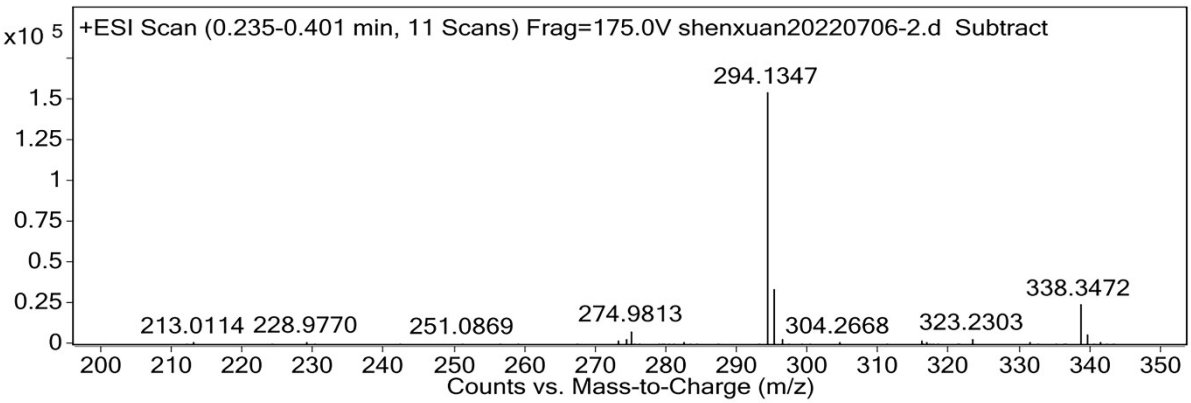

Fig. S9 The ESI-MS spectrum of **pypyr-CH_3**.

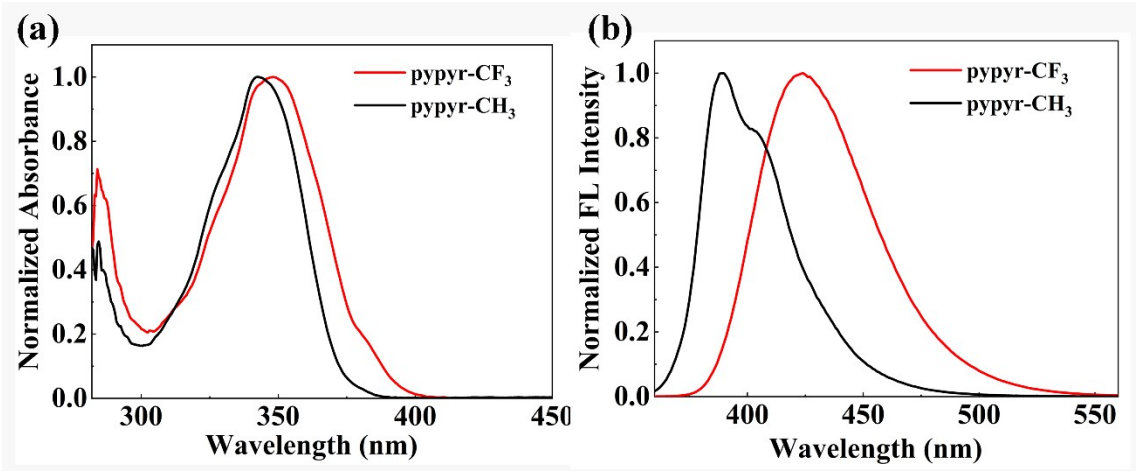

Fig. S10 The UV-Vis absorption (a) and fluorescence (b) spectra of **pypyr-CF_3** and **pypyr-CH_3** in acetonitrile.

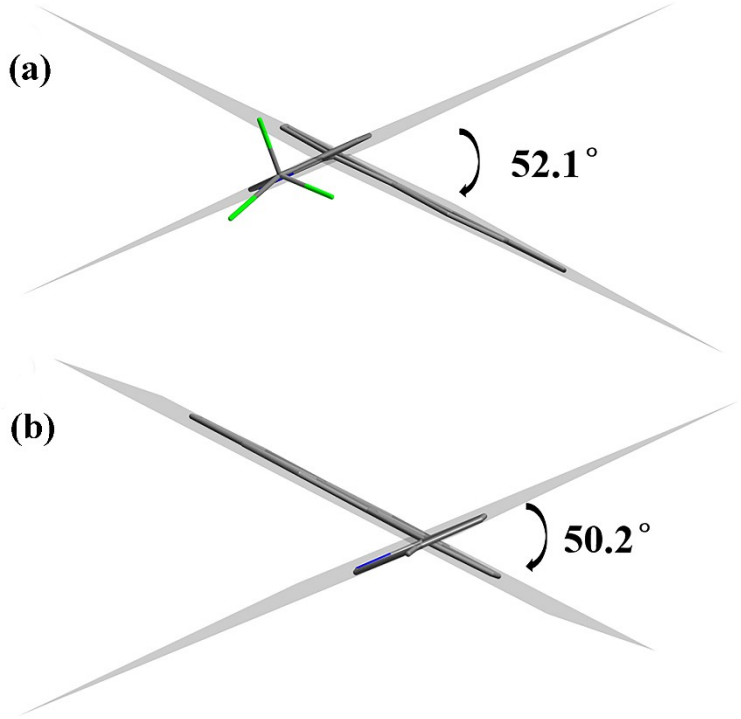

Fig. S11 The dihedral angles in the crystal structures of **pypyr-CF_3** (a) and **pypyr-CH_3** (b).

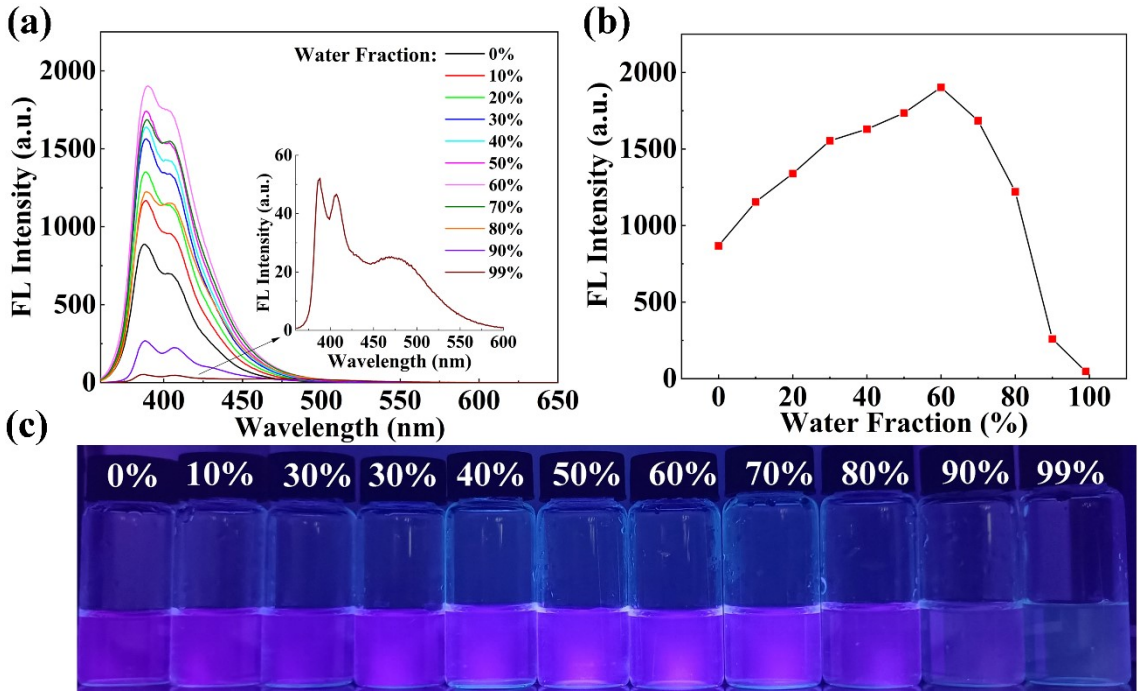

Fig. S12 (a) Fluorescence spectra of **pypyr-CH$_3$** (10 μM) in MeCN/H_2O mixtures with different water fractions; (b) Plots of fluorescence intensity at 390 nm versus water fractions; (c) Photograph of **pypyr-CH$_3$** solution taken under 365 nm UV-lamp.

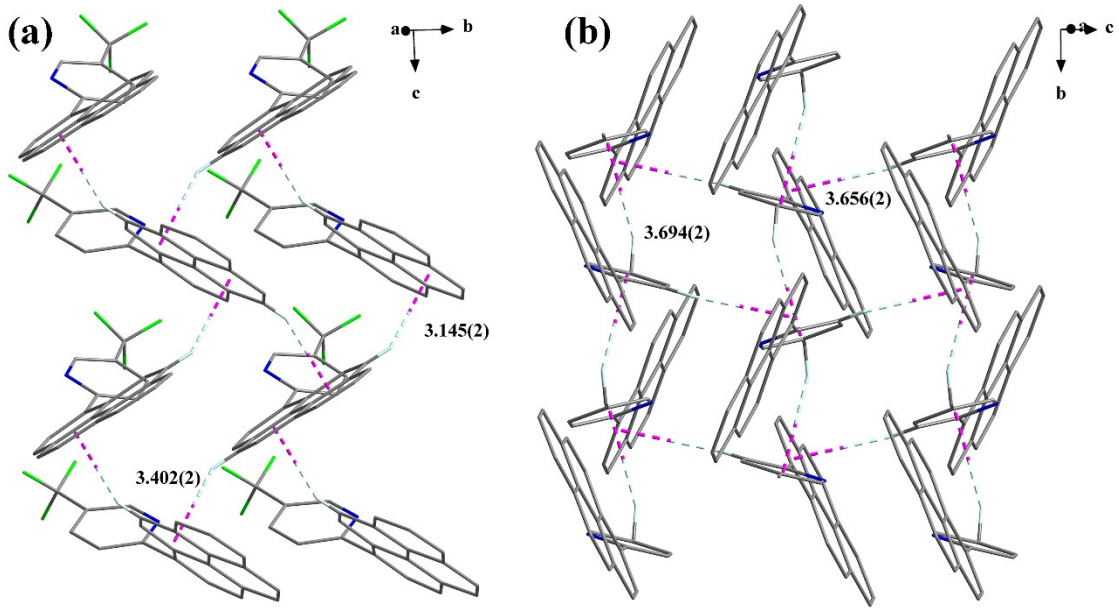

Fig. S13 The packed C-H···π interaction of **pypyr-CF$_3$** (a) and **pypyr-CH$_3$** (b). (H atoms are omitted for clarity)

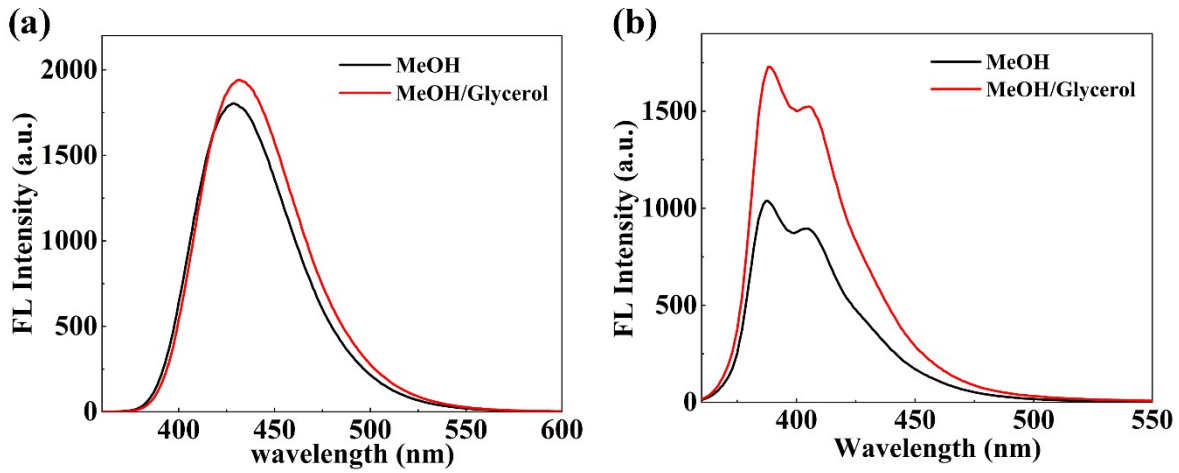

Fig. S14 Fluorescence spectra of (a) **pypyr-CF_3** (10 μM) and (b) **pypyr-CH_3** (10 μM) in pure MeOH or MeOH/Glycerol (7:3) mixture.

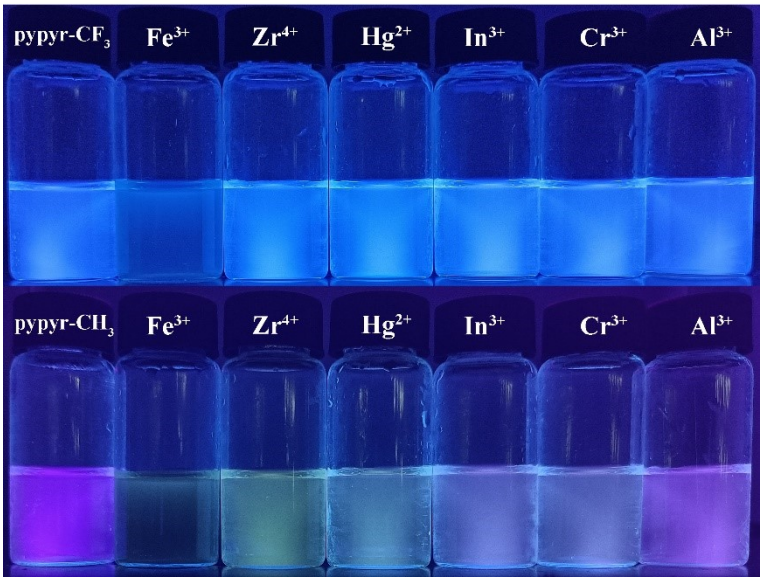

Fig. S15 The photograph of **pypyr-CF_3** and **pypyr-CH_3** (10 μM) in the presence of partial metal ions ([M] = 1 mM) in MeCN/H_2O solution under 365 UV lamp.

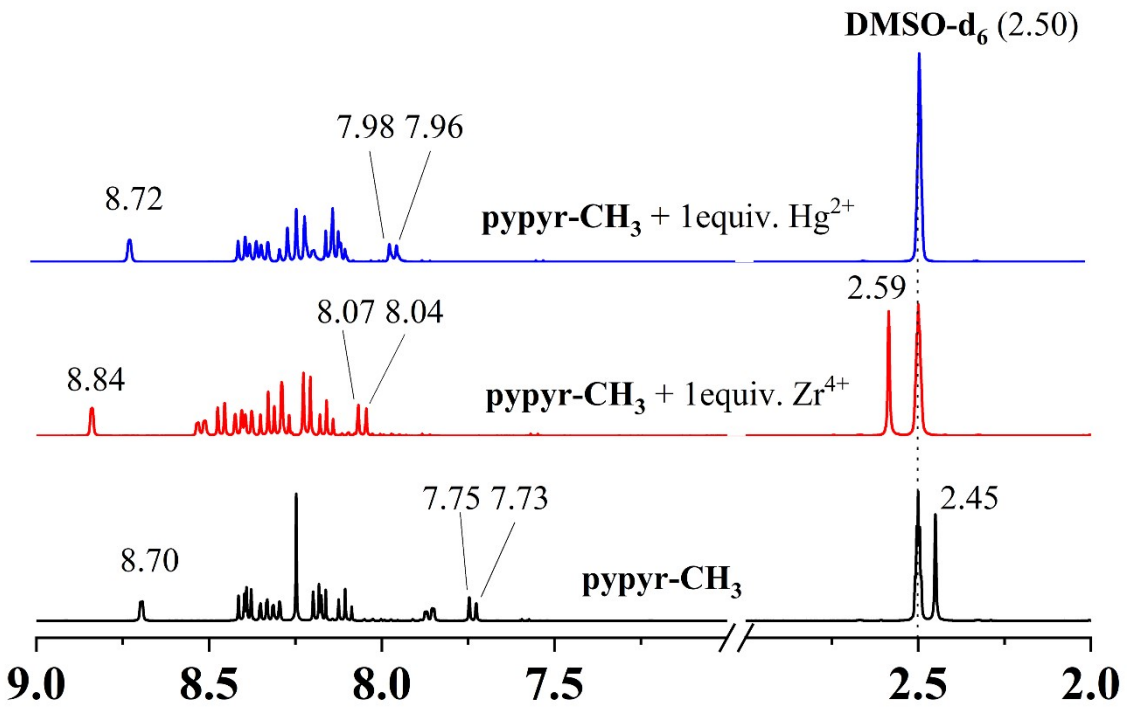

Fig. S16 The ^{1}H NMR spectra **pypyr-CH$_3$** in the absence and presence of Zr^{4+} and Hg^{2+} in DMSO-d_6/D_2O.

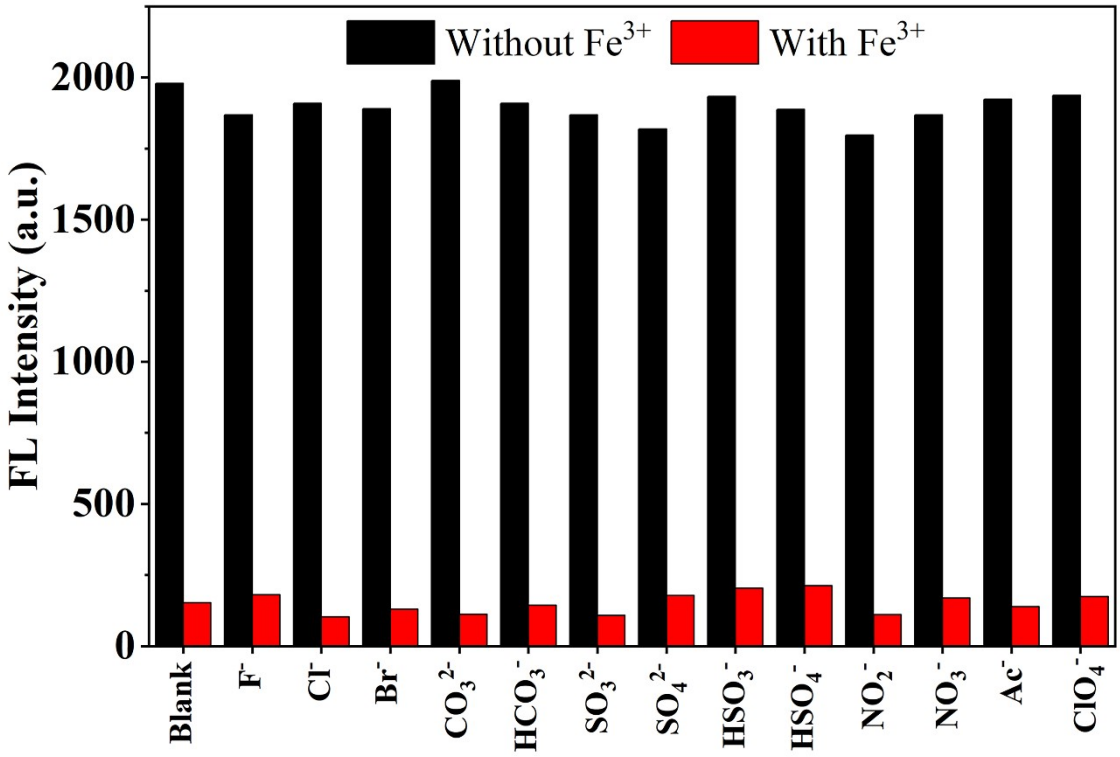

Fig. S17 Fluorescence intensity (λ_{em} = 433 nm) of **pypyr-CF$_3$** (10 μM) in the absence and presence of different anions (1 mM) in MeCN/H_2O (v/v = 7:3, 1 mM Tris-HCl buffer, pH = 7) solution. Black bar represents the response without Fe^{3+}, and red bar indicates the response upon the addition of 100 equiv. of Fe^{3+}.

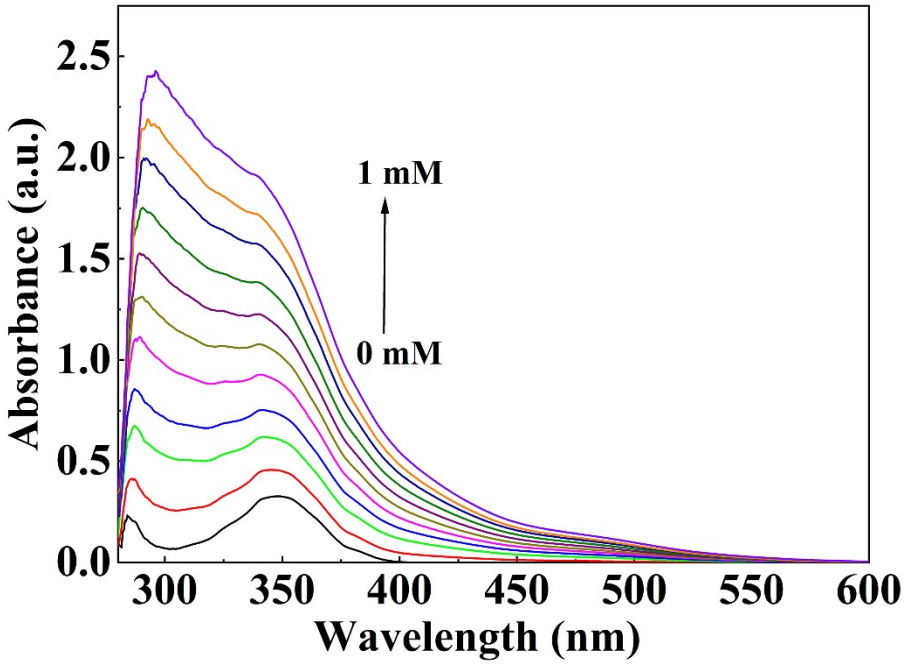

Fig. S18 UV-Vis absorption spectra of **pypyr-CF_3** (10 μM) upon the gradual addition of Fe^{3+} in MeCN/H_2O (v/v = 7:3, 1 mM Tris-HCl buffer, pH = 7) solution.

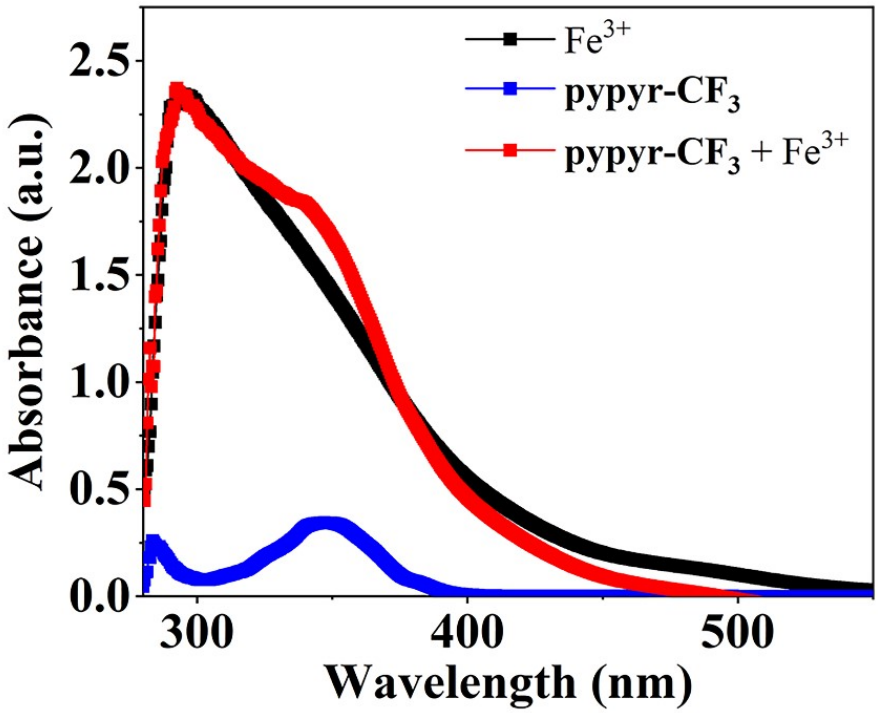

Fig. S19 UV-Vis absorption spectra of Fe^{3+} (1 mM), **pypyr-CF_3** (10 μM) and **pypyr-CF_3** + Fe^{3+} (100 equiv.) in MeCN/H_2O (v/v = 7:3, 1 mM Tris-HCl buffer, pH = 7) solution.

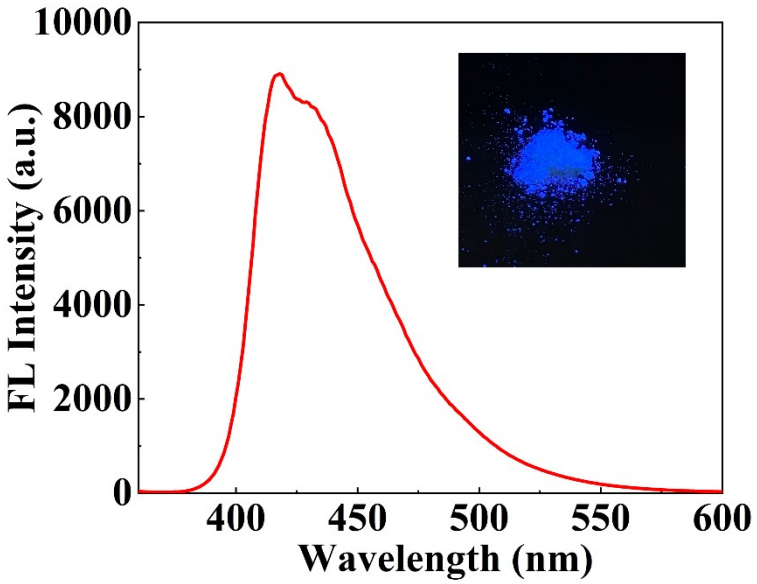

Fig. S20 Fluorescence spectrum of **pypyr-CF_3** in solid state. Inset: photograph of **pypyr-CF_3** in solid state under 365 nm UV lamp.

Table S1 The crystallographic data for **pypyr-CF_3** and **pypyr-CH_3**.

Probes	**pypyr-CF_3**	**pypyr-CH_3**
Empirical formula	$C_{22}H_{12}F_3N$	$C_{22}H_{15}N$
Formula weight	347.33	293.35
Crystal system	Monoclinic	Monoclinic
Space group	$P2_1/c$	$P2_1/c$
a (Å)	26.910(6)	17.626(3)
b (Å)	6.4608(15)	7.6841(13)
c (Å)	9.318(2)	11.574(2)
β (°)	94.442(3)	100.988(2)
V (Å^3)	1615.2(6)	1538.9(5)
Z	4	4
D_c (g·cm^{-3})	1.428	1.266
μ (mm^{-1})	0.108	0.073
F (000)	712	616
Crystal size (mm)	0.19 × 0.13 × 0.11	0.16 × 0.14 × 0.08
θ Range (°)	1.518-24.997	1.177-25.000
Reflections collected	10777	10732
Independent reflections	2841 [R_{int} = 0.0518]	2710 [R_{int} = 0.0448]
Reflections observed [$I > 2\sigma(I)$]	2082	1764
Data/restraints/parameters	2841 / 6 / 235	2710 / 1 / 209
Goodness-of-fit on F^2	1.088	1.023
R_1/wR_2 [$I > 2\sigma(I)$]	0.0566/0.1494	0.0468/0.1103
R_1/wR_2 (all data)	0.0773/0.1598	0.0791/0.1234
Max., Min. $\Delta\rho$ (e·Å^{-3})	0.448, -0.358	0.185, -0.161

Table S2 Patial typical bond lengths (Å) and bond angles (°) for **pypyr-CF_3** and **pypyr-CH_3**.

pypyr-CF_3		**pypyr-CH_3**	
F(1)-C(22)	1.310(4)	N(1)-C(17)	1.341(2)
C(20)-C(22)	1.482(4)	N(1)-C(21)	1.335(2)
N(1)-C(17)	1.343(3)	C(18)-C(19)	1.374(2)
N(1)-C(21)	1.339(3)	C(16)-C(17)	1.487(2)
C(16)-C(17)	1.496(3)	C(20)-C(22)	1.505(2)
C(17)-C(18)	1.379(3)	C(2)-C(3)	1.371(3)
C(21)-N(1)-C(17)	117.0(2)	C(13)-C(14)	1.385(2)
F(2)-C(22)-F(1)	107.0(3)	C(21)-N(1)-C(17)	117.76(15)
C(2)-C(1)-C(10)	121.2(2)	C(2)-C(1)-C(10)	120.91(18)
F(1)-C(22)-C(20)	112.8(3)	C(19)-C(20)-C(22)	122.23(17)